Tectonic and lithologic controls on bedrock channel profiles and processes in coastal California

Alison Duvall[1]
Department of Geological Sciences, University of California, Santa Barbara, California, USA

Eric Kirby
Department of Geosciences, Pennsylvania State University, University Park, Pennsylvania, USA

Douglas Burbank
Department of Geological Sciences, University of California, Santa Barbara, California, USA

Received 29 August 2003; revised 3 May 2004; accepted 21 May 2004; published 20 July 2004.

[1] Recent theoretical models suggest that topographic characteristics of bedrock channels are products of interactions among tectonics, substrate resistance, and the climatically modulated erosive ability of the river. The degree to which these factors influence the form of channel profiles is poorly quantified at present. Here we investigate bedrock channels developed across the southern flank of the Santa Ynez Mountains, California. Uniform climate and systematic variations in lithology and rock uplift rate along the range allow comparison of channel morphology between (1) channels eroding rocks of uniform and nonuniform strength and (2) channels experiencing differences in tectonic forcing. We combine field observations, surveys, and analysis of digital data to determine topographic and hydraulic characteristics of bedrock channels. At a constant rock uplift rate, streams flowing from resistant to less resistant bedrock exhibit highly concave profiles and increased gradients along lower reaches relative to channels developed in uniform bedrock. These effects are interpreted as responses to (1) an increase in substrate resistance to channel incision in the upper reaches and (2) transport-limited gradients along lower reaches. Comparisons of channels developed across uniform lithology but experiencing an approximately sevenfold difference in rock uplift rate reveal an approximately twofold increase in gradient and an approximately threefold decrease in width. In this landscape the combined channel adjustments of gradient and width are consistent with a fluvial incision model in which channel incision rate is linearly proportional to mean bed shear stress. *INDEX TERMS:* 1815 Hydrology: Erosion and sedimentation; 1824 Hydrology: Geomorphology (1625); 8107 Tectonophysics: Continental neotectonics; *KEYWORDS:* bedrock rivers, neotectonics, fluvial geomorphology

Citation: Duvall, A., E. Kirby, and D. Burbank (2004), Tectonic and lithologic controls on bedrock channel profiles and processes in coastal California, *J. Geophys. Res.*, *109*, F03002, doi:10.1029/2003JF000086.

1. Introduction

[2] Rates and patterns of active deformation constitute the basic framework for understanding the geodynamics of deforming lithosphere. Characterizing the spatial distribution of deformation often proves challenging. Even when successful, most field campaigns to define rates and patterns of active deformation provide data (e.g., fault slip rates) for only a few discrete sites within a larger landscape. As a result, developing an improved, quantitative method of gathering tectonic information directly from landscape topography motivates much current research in tectonic geomorphology. Recent studies show that the bedrock channel network dictates critical relationships among relief, elevation, and denudation rate [*Howard*, 1994; *Howard et al.*, 1994; *Whipple and Tucker*, 1999] in tectonically active settings. Moreover, although hillslope form becomes insensitive to increases in uplift rate beyond fairly low values [e.g., *Schmidt and Montgomery*, 1995; *Burbank et al.*, 1996; *Montgomery and Brandon*, 2002], the longitudinal profiles of bedrock rivers may yield valuable information about the distribution of recent deformation within the underlying region. A number of studies have been successful in this regard, using systematic behavior of river profiles to determine patterns of active deformation within a mountain belt [*Hack*, 1957; *Seeber and Gornitz*, 1983; *Keller*, 1986; *Merritts and Vincent*, 1989; *Lavé and Avouac*, 2000, 2001]. Quantitative realizations of this goal, however, remain limited to field sites where local calibration of model parameters is possible [*Kirby and Whipple*, 2001].

[1]Now at the U.S. Geological Survey, Menlo Park, California, USA.

0148-0227/04/2003JF000086$09.00

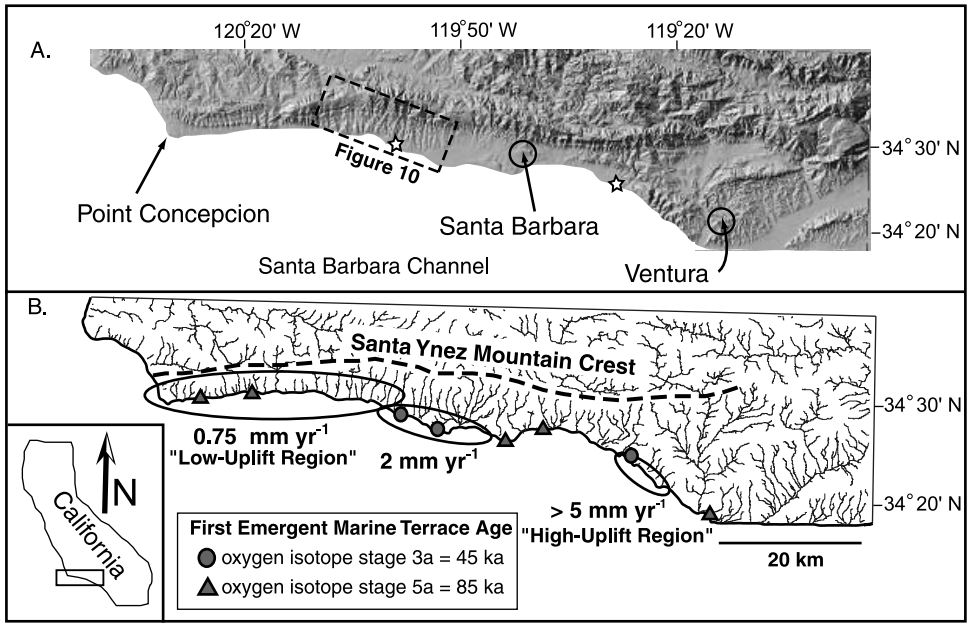

Figure 1. Location of study along the Santa Ynez Mountains. (a) Relevant stream channels and geographic landmarks of the field site. The small dashed box shows the area of Figure 10. Stars indicate weather station locations (Santa Barbara County Flood Control District) for climate data reported in Table 5. (b) Drainage network and crest of the Santa Ynez Mountains. Triangle and circle symbols indicate locations and marine isotopic stages (stage 3a $\approx$ 45 ka, 5a $\approx$ 85 ka) of dated first-emergent marine terraces [*Metcalf*, 1994; *Trecker et al.*, 1998]. Rock uplift rates derived from marine terrace data are also shown. Note that rock uplift rates are low ($\sim$0.75 mm yr^{-1}) in the west ("low-uplift region") relative to the high rate toward the east near Ventura ($\sim$5 mm yr^{-1}) ("high-uplift region"). The inset shows the regional extent of the study area.

[3] To a large degree, this limited success reflects our incomplete understanding of the dynamics of bedrock incision by flowing water and moving sediment. Unlike alluvial rivers, bedrock channel incision processes have only recently received focused attention [*Howard and Kerby*, 1983; *Hancock et al.*, 1998; *Sklar and Dietrich*, 1998; *Tinkler and Wohl*, 1998; *Snyder et al.*, 2000; *Whipple et al.*, 2000a; *Kirby and Whipple*, 2001]. To date, multiple models for reach- and time-averaged bedrock incision have been proposed [see *Whipple*, 2004]; most of these fall into a stream power family in that they parameterize bedrock incision as a function of observable topographic characteristics, such as drainage area and channel gradient [*Whipple*, 2004]. Both the simplicity and physically based nature of this class of models generate wide appeal, and they have been used in numerous numerical simulations of landscape evolution [*Anderson*, 1994; *Howard*, 1994; *Tucker and Slingerland*, 1996; *Willett*, 1999]. Data to calibrate various model parameters, however, are sparse [*Howard and Kerby*, 1983; *Seidl and Dietrich*, 1992; *Stock and Montgomery*, 1999; *Snyder et al.*, 2000; *Whipple et al.*, 2000a; *Kirby and Whipple*, 2001], and discriminating tests of competing models are few [*Tomkin et al.*, 2003; *van der Beek and Bishop*, 2003]. Our ability to extract tectonic information directly from channel profiles requires a quantitative understanding of relationships among such factors as channel gradient, channel width, substrate rock strength, and rock uplift rate. Progress toward this goal, however, has been incremental, due in large part to the difficulty of isolating the influence of various factors in field-based studies [e.g., *Snyder et al.*, 2000].

[4] In this study, inspired by an interest in extracting tectonic information directly from stream profiles, we exploit systematic variations in rock uplift rate and rock mass quality within the Santa Ynez Mountains of California to assess the manner and degree to which bedrock channels respond to variations in rock strength and tectonic forcing. The uniform coastal climate allows us to isolate both influences on the development of bedrock channels. Furthermore, we utilize the coupled response of channel gradient and width to differences in rock uplift rate within this field site to place bounds on acceptable model parameters.

2. Santa Ynez Mountains Field Site

[5] The Santa Ynez Mountains of coastal southern California (Figure 1) are a topographically rugged south dipping homocline with a maximum elevation of 1400 m [*Dibblee*, 1982; *Tierney*, 2002]. The study area includes $\sim$70 dominantly bedrock channels (Figure 2), which incise the southern flank of the range. In general, channel morphology alternates between prominently bedrock reaches characterized by exposures of underlying units along channel bottoms and walls (Figures 3a and 3b) and "mixed" sections, where bedrock channel bottoms and/or walls are covered by a thin and scattered blanket of coarse alluvium (Figure 3c). Exceptions occur at the very top of drainages (colluvial hollows dominated by debris flows) and through

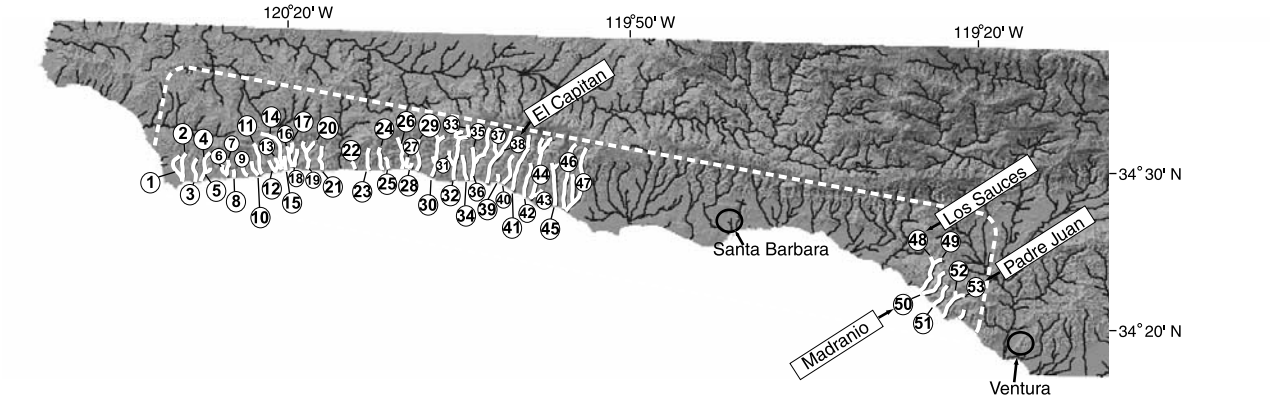

Figure 2. Drainage network of the Santa Ynez Mountains. Streams used in study calculations are numbered and are outlined in white. Channels observed in the field are labeled by stream name.

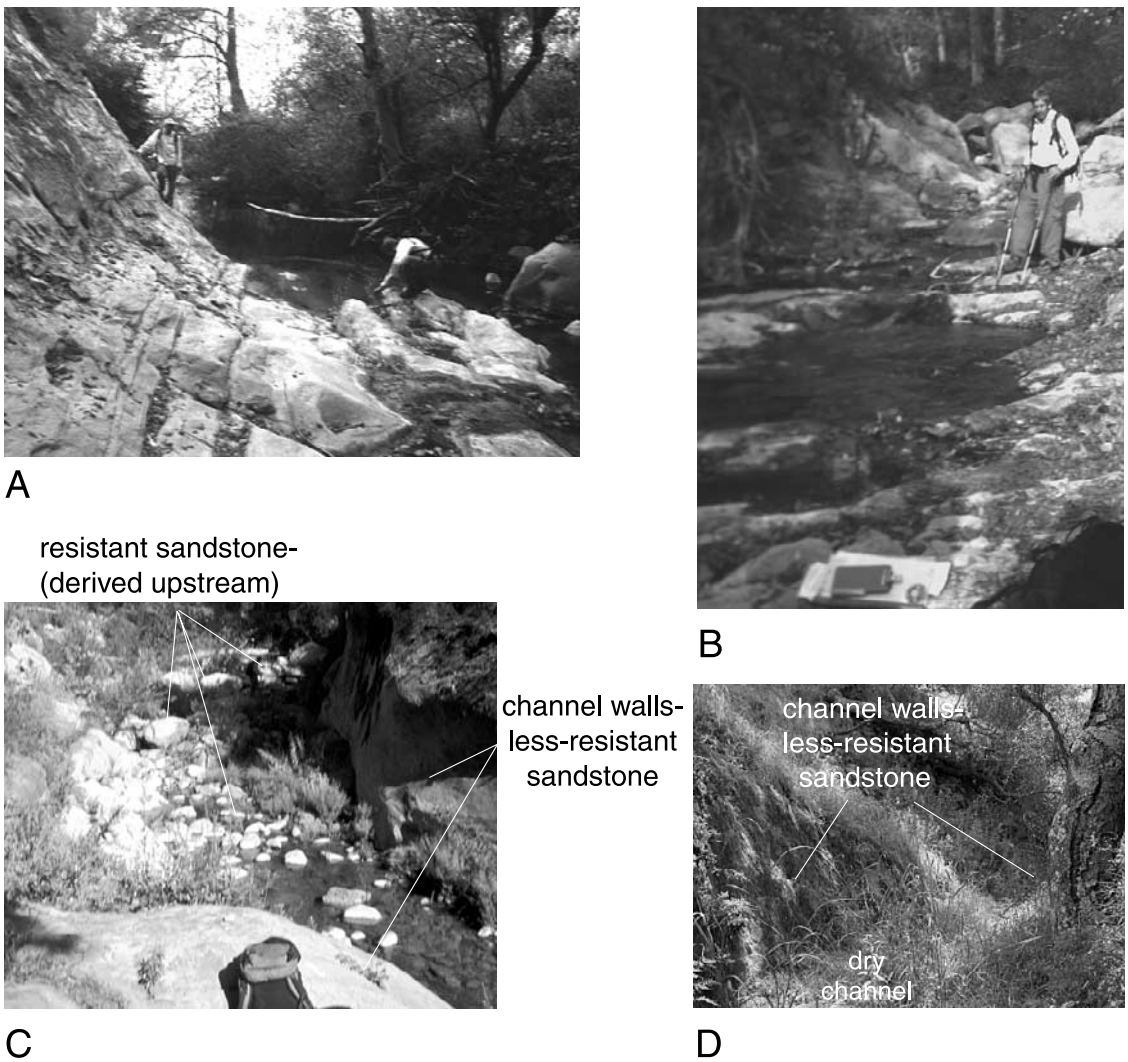

Figure 3. Field photos taken within study area channels. (a, b) Examples of resistant bedrock-dominated reaches within El Capitan stream (number 38) (Figure 2). (c) Example of "mixed" reach in the same channel. Note the scattered blanket of coarse alluvium and especially the larger cobbles and boulders derived from the resistant bedrock upstream. The obvious bedrock channel walls are less resistant Vaqueros sandstone. (d) Example of a channel carved in less resistant bedrock with no influence of resistant boulders from upstream (channel begins below the transition in rock strength). The photograph was taken during the dry season in a tributary to El Capitan stream.

Table 1. Stream Channel Data

Channel Name	Channel Length, km	Drainage Area, km^2	Identification Number[a]	θ[b]	k_{sn}[c]
Low-Uplift Region: Uniform Rock Strength[d]					
Canada del Gato	4	2.5	6	0.58 ± 0.06	18
Canada del Coyote	3.4	0.5	15	0.35 ± 0.11	8.75
Canada de Gallina	1.1	0.2	25	0.48 ± 0.46	14.2
Canada de la Huerta	1.4	0.4	27	0.41 ± 0.09	13.1
Canada de la Pila	3.2	1.5	28	0.67 ± 0.07	19
Aguajito Canyon	6.4	12	31	0.53 ± 0.05	15.8
Venadito Canyon	6.2	6	34	0.40 ± 0.06	10.6
Canada del Destiladera	3.6	2.5	39	0.34 ± 0.07	13.9
Mean (standard error)	**3.7**	**3.2**		**0.48 ± 0.04**	**13.8 ± 4.0**
Low-Uplift Region: Nonuniform Rock Strength[d]					
Wood Canyon (west)	7.4	5	1	0.97 ± 0.15	11.3
Wood Canyon (east)	6.6	7	2	0.51 ± 0.12	14.2
Damsite Canyon	6	4.5	3	1.6 ± 0.26	16.5
Canada del Cojo	7	9	4	0.65 ± 0.10	19.3
Canada del Cementerio	4.6	2.5	5	0.62 ± 0.13	11.6
Barranca Hondo	4.9	3	7	1.1 ± 0.11	23.5
Canada de la Llegua	4.5	2.5	8	0.87 ± 0.09	17
Arroyo San Augustin	5.2	5.5	9	0.85 ± 0.06	21.7
Canada del Pescado	3.9	1.5	10	0.74 ± 0.10	13.6
Canada de las Agujas	5.4	4	11	0.87 ± 0.09	18.4
Arroyo el Bulito (west)	7	7.5	12	1.8 ± 0.30	21.4
Arroyo el Bulito (east)	6	7	13	2.1 ± 0.30	22.6
Canada del Agua	4.6	3.5	14	0.89 ± 0.11	16.1
Canada del Sacate (west)	4.6	4.5	16	0.72 ± 0.06	18.5
Canada del Sacate (east)	4.6	4.5	17	0.86 ± 0.08	19.3
Canada de Cuarta	5.2	5	18	0.92 ± 0.10	18.7
Canada de Alegria (west)	6.2	10	19	0.54 ± 0.06	17.9
Canada de Alegria (east)	6	10	20	0.6 ± 0.06	17.1
Canada del Agua Caliente	6	8	21	0.55 ± 0.08	14.8
Canada San Onofre	4.6	6.5	22	0.38 ± 0.01	53.3
Canada del Molino	5.4	4.5	23	1.2 ± 0.14	39.8
Canada de la Posta	4	3	24	0.71 ± 0.13	38.9
Arroyo Hondo	6.2	10.5	26	0.40 ± 0.06	37.7
Arroyo Quemado	6.3	9	29	1.9 ± 0.12	40.1
Tajiguas Creek	8.9	12	30	1.6 ± 0.22	21.5
Canada del Refugio	8	12	32	1.2 ± 0.14	32.4
Refugio east fork	10	12	33	0.90 ± 0.14	47.5
Las Flores Canyon	7	4	35	0.76 ± 0.06	21.4
Canada del Corral	10.5	11	36	0.58 ± 0.05	43.8
El Capitan Canyon (west)	9.5	12.5	37	0.97 ± 0.11	51.9
El Capitan Canyon (east)	10.2	12.5	38	0.81 ± 0.03	34.5
Las Llagas Canyon	6.3	8.5	40	0.77 ± 0.08	22.7
Gato Canyon	10.7	10	41	0.88 ± 0.06	39.3
Las Varas	7.5	9	42	0.69 ± 0.04	20.9
Dos Pueblos (lower fork)	12	9	43	0.54 ± 0.06	10.9
Dos Pueblos (east)	12.1	11	44	0.55 ± 0.07	46.7
Mean (standard error)	**7**	**7.5**		**0.92 ± 0.07**	**26.5 ± 2.1**
High-Uplift Region: Uniform Rock Strength[d]					
Los Sauces Creek (west)	8.5	3.5	48	0.37 ± 0.06	24.1
Los Sauces Creek (east)	8.5	9	49	0.56 ± 0.07	19.7
Madranio Creek	5.2	7.5	50	0.54 ± 0.06	29.4
Javon Canyon	6.3	8	51	0.55 ± 0.12	27
Padre Juan (west)	6.9	9	52	0.58 ± 0.05	25.4
Padre Juan (east)	6.9	9	53	1 ± 0.06	30.9
Mean	**7.1**	**7.7**		**0.6 ± 0.09**	**26.1 ± 4.9**

[a]See Figure 2 for stream locations.
[b]Channel concavity or curvature of the longitudinal profile.
[c]Normalized steepness index calculated for each stream using a reference concavity of 0.4.
[d]Low-uplift region $\cong$ 0.75 mm yr^{-1}; high-uplift region $\cong$ 5 mm yr^{-1}.

lower alluvial reaches near to the channel outlet. The subparallel channels are generally steep, narrow, and short, with an average channel length of 6.4 km. Drainage areas vary from 0.2 to 12.5 km^2, with an average of 6.5 km^2 (Table 1). The study area has a Mediterranean climate characterized by episodic, cool winter storms and a warm, dry spring, summer, and fall.

[6] Flights of marine terraces are present along the length of the study area coastline. Previous studies in the western [*Metcalf*, 1994; *Gurrola et al.*, 1998] and eastern parts of the range [*Trecker et al.*, 1998] developed an extensive chronology of these well-preserved marine terraces. Terraces within the field site have been dated using a variety of chronologic techniques [*Rockwell et al.*, 1992;

Metcalf, 1994; *Gurrola et al.*, 1998; *Trecker et al.*, 1998] and correlated with the most recent eustatic sea level curve [*Lambeck and Chappell*, 2001] in order to define the rates and patterns of rock uplift. Thus in this study, "rock uplift" refers to vertical motion of rock with respect to modern sea level. Pleistocene rock uplift rates vary considerably along a 125 km transect, from $\sim$0.75 mm yr^{-1} in the western part of the range to $\sim$5 mm yr^{-1} at Red Mountain near Ventura (Figure 1) [*Metcalf*, 1994; *Gurrola et al.*, 1998; *Trecker et al.*, 1998]. Despite these strong lateral gradients in rock uplift rate, the elevations of multiple terrace levels at a site are consistent with little temporal variation in rock uplift over the past $\sim$200 kyr [*Metcalf*, 1994]. In addition, terrace treads dip consistently $\sim$2°–4° seaward, suggesting minimal variations in rock uplift between the coast and range crest [*Metcalf*, 1994].

[7] Bedrock exposed in study area channels consists of an assemblage of Eocene through Pliocene sedimentary rocks [*Dibblee*, 1982]. Rock units exposed along the flank of the homocline strike nearly east–west, parallel to the range crest. As a consequence, the pattern of lithologic variations is nearly constant along the strike of the range. In the western study area (low rock uplift), exposures of resistant (Eocene) sandstone crop out along the range crest and upper mountain flanks. These resistant beds stand in contrast to the soil-mantled hillslopes developed in the less resistant (Oligocene-Pliocene) sandstone, conglomerate, and shale along the lower flanks of the range. Of particular utility for this study, a small subset of channels is developed entirely within these less resistant rocks. In contrast, none of the channels in the eastern (high rock uplift) region cross major transitions in rock strength. In this site, channels erode only the relatively weak Oligocene-Pliocene units.

[8] The Santa Ynez Mountains provide a favorable location to study bedrock channel erosion because channel response to variability in both rock strength and rock uplift rate can be examined in isolation. The presence of streams that flow through uniform substrate interspersed among streams that encounter a major rock strength transition provides the opportunity to examine effects of variations in lithologic erodibility on the channel profile. The same "weak rock–only" channels can also be compared to similar channels experiencing a much higher rate of rock uplift, which provides quantitative insights regarding channel response to tectonic forcing.

3. Models for Bedrock Incision

[9] Empirical studies of bedrock channel gradients in a variety of field settings typically reveal a scaling between local channel slope and upstream drainage area [*Hack*, 1957; *Flint*, 1974; *Howard and Kerby*, 1983] of the form

$$S = k_s A^{-\theta}, \tag{1}$$

where S is the local channel gradient, A is the contributing drainage area, and k_s and θ are parameters which describe the relative steepness and concavity of the channel, respectively. As previous studies have shown, simple models for both detachment-limited and transport-limited bedrock incision predict power law relations between channel gradient and drainage area similar in form to equation (1) [*Howard*, 1994; *Howard et al.*, 1994; *Willgoose*, 1994; *Whipple and Tucker*, 1999]. These models further predict that (1) the concavity index (θ) is independent of rock uplift rate and that (2) a power law relationship exists between the steepness index (k_s) and rock uplift rate. Thus as developed in recent theoretical studies [e.g., *Whipple and Tucker*, 1999], topographic analyses of channel profiles can, in principle, place bounds on model parameters.

[10] Despite preliminary support for these predictions [*Snyder et al.*, 2000; *Kirby and Whipple*, 2001], factors omitted from simple models may complicate the quantitative relations between channel topography and incision rate. These factors include (1) adjustments to channel width and/or sinuosity [*Harbor*, 1998; *Lavé and Avouac*, 2000, 2001], (2) variations in the hydraulic roughness, bed material grain size, and/or extent of alluvial cover [*Sklar and Dietrich*, 1998, 2001; *Whipple and Tucker*, 2002], (3) nonlinearities in the incision process, including thresholds for detachment of bed material [*Whipple and Tucker*, 1999; *Tucker and Bras*, 2000; *Snyder et al.*, 2003b], (4) frequency of debris flows [*Stock and Dietrich*, 2003], and (5) orographic influences on the distribution of precipitation [*Roe et al.*, 2002, 2003]. Acknowledging these potential complications, we wish to evaluate to what degree a simple channel incision rule can explain profile characteristics in a field setting where a few of the key variables can be studied in isolation.

3.1. Model Derivation

[11] Most formulations of fluvial incision into bedrock begin with the postulate that erosion rate (E) is a power law function of mean bed shear stress (τ_b) beyond a critical threshold (τ_c):

$$E = k_e(\tau_b - \tau_c)^a, \tag{2}$$

where k_e is a dimensional coefficient and a is a positive constant which depends on incision process [e.g., *Hancock et al.*, 1998; *Whipple et al.*, 2000a]. Recognizing that the derivation of such models has become relatively common [*Seidl and Dietrich*, 1992; *Howard*, 1994; *Whipple and Tucker*, 1999; *Snyder et al.*, 2000, 2003a] but acknowledging the utility of a theoretical framework, we present a full derivation in Appendix A. Interested readers are referred to reviews by *Whipple and Tucker* [1999, 2002] and *Whipple* [2004].

3.2. Previous Studies of Model Parameters

[12] Because multiple variables are encompassed in the erosion coefficient (K) (equation (A5)), several factors influence K, including, but probably not limited to, channel width, rock strength, channel bed material, and runoff (climate controlled) [*Sklar and Dietrich*, 1998, 2001; *Stock and Montgomery*, 1999; *Snyder et al.*, 2000, 2003a]. Only a few recent studies have documented K values [*Howard and Kerby*, 1983; *Rosenbloom and Anderson*, 1994; *Seidl et al.*, 1994; *Stock and Montgomery*, 1999; *Kirby and Whipple*, 2001]. One study of bedrock river incision [*Stock and Montgomery*, 1999] shows that K can scale over orders of magnitude due to variability in rock strength and/or climate among field sites. Other recent studies conducted in the King Range in northern California [*Snyder et al.*, 2000,

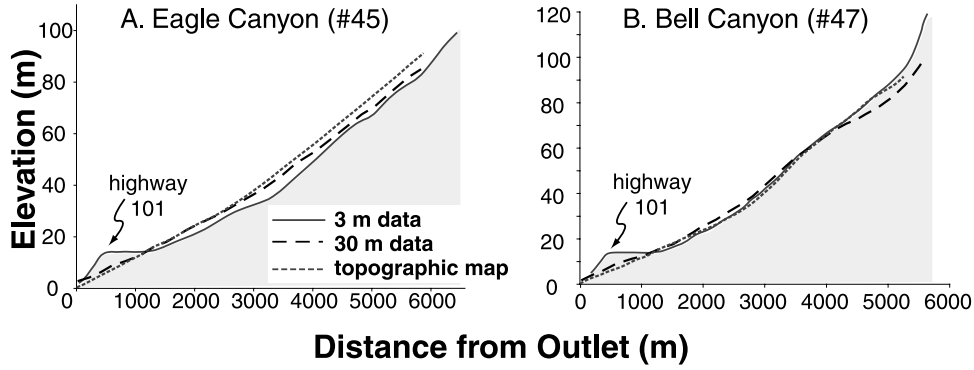

Figure 4. Comparison of digital elevation model accuracy between the 3 m data set, the 30 m data set, and the USGS 7.5 min quadrangle topographic map. Profile data from the lower reaches of two Santa Barbara area channels (numbers 45 and 47) (Figure 2) were used in this comparison. The 3 m data set picks up anthropogenic features, and we interpret the irregularity in lower profiles as such. Data shows that the 30 m data set captures key topographic features of the channel profiles.

2003a, 2003b] suggest that the coefficient of erosion varies in concert with rock uplift rate due at least in part to feedbacks between topography, orographic precipitation, and thresholds in the processes of channel incision. That tectonic rates could affect the coefficient of erosion (K) is a significant outcome given that many researchers commonly hold K constant in areas of uniform rock type and, in doing, so make the assumption that channel gradient is the only variable free to adjust to tectonic forcing [*Whipple and Tucker*, 1999].

[13] The fundamental role of the slope exponent (n in equation (A5)) in dictating the relationship between rock uplift rate, equilibrium channel slope, and the height of mountain ranges has recently been emphasized [*Whipple and Tucker*, 1999]. Despite the importance of this parameter [*Whipple and Tucker*, 1999], actual field-calibrated values for this exponent are few [*Howard and Kerby*, 1983; *Snyder et al.*, 2000; *Kirby and Whipple*, 2001]. Scaling arguments suggest that the slope exponent, n, should depend on the dominant erosion process and should fall somewhere between $\sim$2/3 and $\sim$5/3 for plucking, macroabrasion, and abrasion by suspended load [*Hancock et al.*, 1998]. *Howard and Kerby* [1983] reported $n \sim 2/3$ in a seminal study of bedrock river erosion in the badlands of Virginia. More recently, workers have documented bedrock erosion consistent with n values between 2/3 and 1 in the Nepalese Siwaliks [*Kirby and Whipple*, 2001] and <1 in south central Alaska [*Whipple et al.*, 2000b]. The range of n values extracted from previous field studies underscores the need for further investigation of the degree to which this model parameter varies among field sites.

4. Methods

4.1. Stream Profile Analysis

[14] For each of 50 streams along the coast (Figure 2) we extract topographic parameters, including channel longitudinal profiles (stream-wise distance and elevation) and contributing drainage area, from a digital elevation model (DEM).

4.1.1. Channel Longitudinal Profiles

[15] Channel profiles were extracted from a U.S. Geological Survey (USGS) 30 m DEM generated from 7.5′ topographic maps. DEMs are the simplest and most effective template for creating basin-wide drainage area data sets [*Snyder et al.*, 2000]. Because the profile is extracted digitally, however, accuracy is limited by the resolution of the DEM. Thirty meter data, although readily available, might be considered too coarse for characterizing small catchments, such as those in the Santa Ynez Mountains. To assess the validity of our 30 m data set, we conducted a comparison between it, higher-resolution 3 m DEM [*Keller and Gurrola*, 2000] data covering a portion of our study area within the cities of Santa Barbara and Goleta, and profiles generated by hand from 1:24,000 scale USGS topographic maps. A reasonable coincidence between all three profiles (Figure 4) demonstrates that the 30 m data set captures the essential channel geometric characteristics. Although reach slopes may vary in a given data set, the key slope variable used in this study is an integrated slope along the fluvial channel, for which the variation in slope among data sets is <1%.

[16] In order to minimize inherent scatter in the elevation points along the stream profile (a consequence of DEM generation and data processing (see C. Wobus et al. (Tectonics from topography: Procedures, promise and pitfalls, submitted to *GSA Special Publications*, 2003, hereinafter referred to as Wobus et al., submitted manuscript, 2003) for a discussion), we filter the elevation data by passing a moving average along the raw channel elevations (window size of 750 m). Local channel slopes are then calculated from the smoothed data using a constant vertical interval (ΔZ) of 5 m, close to the contour interval of the topographic data from which the DEM is derived. This type of sampling yields a data set evenly distributed in log S-log A space (Wobus et al., submitted manuscript, 2003) in contrast to calculating slopes at equal length intervals (ΔL), which tends to concentrate data in the lower channel reaches.

4.1.2. Slope Area Analysis

[17] Following methods developed by *Snyder et al.* [2000] and *Kirby et al.* [2003] and discussed in detail by Wobus et al. (submitted manuscript, 2003), we compile elevation, distance, and drainage area data for each channel by utilizing a group of built-in functions in ARC/INFO. Power law regression analysis of river slope against drain-

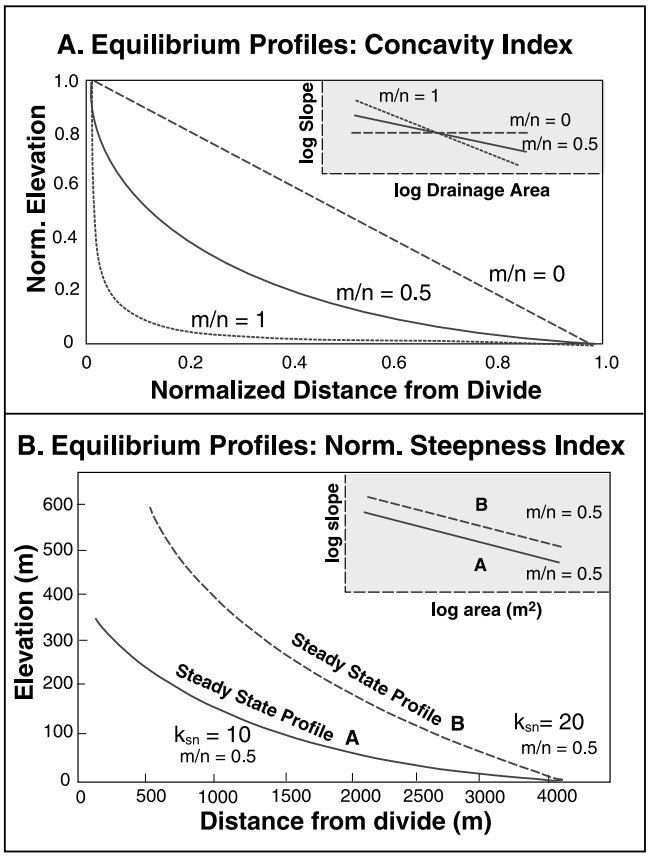

Figure 5. Schematics of key parameters derived from equilibrium longitudinal profiles [modified from *Whipple and Tucker*, 1999]. (a) Longitudinal stream profile concavity is set by the *m*/*n* ratio (concavity index). The upper inset shows different *m*/*n* values in slope-area space, and the main graph shows the same three ratios in elevation-distance space. (b) Two profiles with varying steepness indices. Note that although stream B is twice as steep as stream A, they have the same concavity.

age area using MATLAB scripts and an Arcview interface yields both the channel concavity (θ) and a relative estimate of the steepness index referred to as the normalized channel steepness index (k_{sn}) (equation (1), Figure 5). In general, scaling breaks interpreted to mark the transition between hillslope or colluvial channels and the fluvial channel network can be identified in topographic data by an abrupt decrease in channel slope with increasing drainage area (Figure 6). Although we might expect a gradual transition between these regimes as a consequence of erosive debris flows [e.g., *Stock and Dietrich*, 2003], we restrict the analysis to regions downstream of readily defined breaks in scaling (Figure 6).

[18] Following *Snyder et al.* [2000] and *Whipple* [2004], a fixed reference concavity (θ_r) was used to calculate a normalized steepness index (k_{sn}). Use of a reference concavity overcomes the inherent correlation of regression slope and intercept in equation (1) and facilitates comparison of gradients on channels with widely varying drainage areas [e.g., *Kirby et al.*, 2003]. For any given channel profile the numerical value of the normalized steepness index is a function of the reference concavity. Because we are interested in spatial variations in channel characteristics, the relative, rather than absolute, value of steepness index is most significant. A simple sensitivity experiment with reference concavities spanning a wide range (0.2–0.7) indicates that despite a 1000-fold change in normalized steepness index for a given stream, the ratio of indices between two streams changes <2% (Table 2). Hence for our purposes we consider the relative steepness index or steepness ratio to be independent of the chosen reference concavity.

4.2. Field Data

[19] Although private ownership severely restricts access to most channels along the Santa Ynez coast, we were able to gain entry to the entire El Capitan watershed in the western study area and to three watersheds in the eastern region: Los Sauces, Madranio, and Padre Juan (Figure 2). In each watershed, data were collected on rock strength along the stream length, high-flow channel width, and general channel characteristics, such as size and sorting of sediment and active channel scour.

4.2.1. Rock Competence Survey

[20] Variations in rock type, or more specifically, rock competence, play an important role in setting bedrock incision rates [*Hack*, 1957; *Stock and Montgomery*, 1999; *Whipple et al.*, 2000a, 2000b; *Sklar and Dietrich*, 2001]. Intact rock strength was measured in the field with a Schmidt hammer in order to assess variations in rock resistance along the channel length. Such Schmidt hammer field measurements are comparable to measurements of unconfined compressive strength conducted in a laboratory

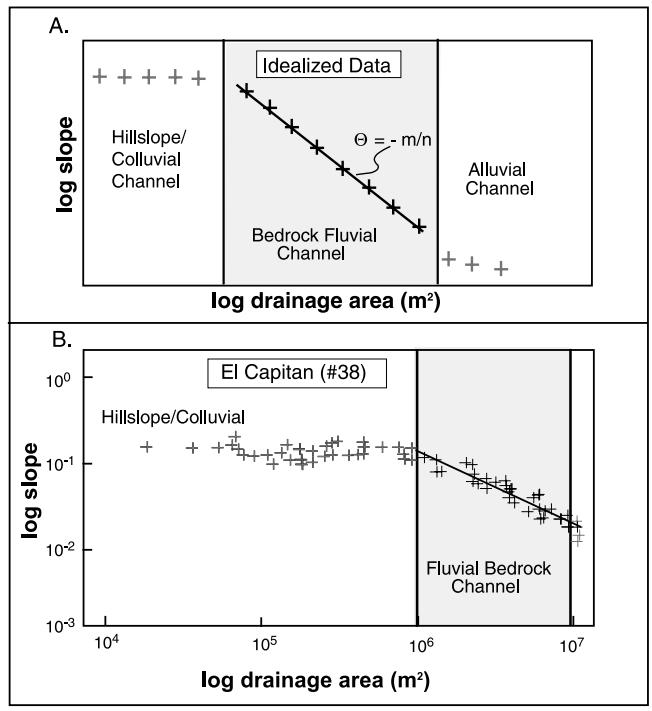

Figure 6. Interpretations of slope-area data for both (a) an ideal data set and (b) El Capitan (number 38) (Figure 2). Note that the obvious break in slope indicates the beginning of fluvial channels.

Table 2. Reference Concavity Comparison[a]

Venadito Canyon (θ = 0.4)		Javon Canyon (θ = 0.54)	
Reference Concavity	Steepness Index (k_{sn1})	Steepness Index (k_{sn2})	Ratio (k_{sn2}/k_{sn1})
0.2	0.592	1.58	2.67
0.3	2.46	6.61	2.69
0.4	**10.4**	**27.8**	**2.67**
0.5	44.1	117	2.65
0.6	186	488	2.62
0.7	781	2050	2.62

[a]Boldface indicates the reference concavity (0.4) used in this study.

[*Selby*, 1982]. Typically, we collected 40–60 individual measurements of the least fractured rock surface per site for all rock units exposed along the surveyed channel reach (Table 3). We omitted any test that yielded a hollow-sounding impact, fractured the rock, or yielded a value <11 because the minimum instrument reading is 10. In addition, no correction was made for the inclination of the hammer because this correction becomes negligible when large numbers of measurements with significant scatter are collected [*Snyder et al.*, 2003b].

4.2.2. Channel Width

[21] As rivers adjust to spatial or temporal variations in vertical tectonic rates, channel width is likely to be an adjustable channel parameter [*Lavé and Avouac*, 2000; *Schumm et al.*, 2000; *Hancock and Anderson*, 2002]. A narrower channel should, in theory, focus more erosive energy on a smaller part of the bed, thereby facilitating more rapid incision. Consequently, in our study area, some channel narrowing might be expected in the high-uplift streams. Detailed field surveys of high-flow channel width were carried out in this field site in order to document width variations.

[22] Classically, hydraulic geometry relations describe a downstream trend in channel width (w) with discharge (Q):

$$w = k_w Q^b, \tag{3}$$

where k_w is a dimensional coefficient, b is the width-scaling exponent, and Q is considered the dominant or "channel forming" discharge. Although originally defined by an empirical relationship observed in alluvial rivers [e.g., *Leopold and Maddock*, 1953], similar scaling relations have been observed in bedrock rivers [*Montgomery and Gran*, 2001].

[23] Because discharge data were not available for small streams in this field site, drainage area was used as a proxy for discharge, and regression analyses were performed on width versus drainage area data [after *Snyder et al.*, 2000, 2003a]. When drainage area is used in place of discharge, equation (3) is rewritten as

$$w = k_w k_q^b A^{cb} = k'_w A^{b'}, \tag{4}$$

where $k_q^b A^c = Q$.

[24] We combined digitally derived drainage area data with field measurements of channel width to establish the general relationship between width and drainage area for both a high-uplift and a low-uplift stream. More specifically, we compared the width-scaling exponent (b') and the width coefficient (k'_w) between a tributary to El Capitan stream in the low-uplift region and Madranio creek in the high-uplift region (Figure 2). We examined a tributary to El Capitan rather than the main trunk stream because the main channel crosses a pronounced transition in rock strength (see section 5.1), whereas the tributary stream flows entirely through weak substrate (Table 3). Thus these streams provide an opportunity to isolate the effects of rock uplift rate on channel width, independent of lithologic influences.

[25] Given the difficulty of defining a channel-forming discharge in bedrock channels, we defined channel width as the zone of recently active erosion (considered roughly equivalent to "bankfull width" in alluvial rivers). Typically, this was marked by obvious scour of bedrock, breaks in slope, and an absence of vegetation/moss [*Snyder et al.*, 2003b]. Wherever possible, measurements of width were taken between bedrock exposures defining both margins of the channel. In the context of observed reach-scale variations in bedrock competence, widths were consistently measured within locally resistant units: Such units impose upper limits on channel erodibility and ultimately dictate the overall channel geometry.

5. Results

5.1. Rock Strength

[26] In order to assess bedrock competence, over 1000 Schmidt hammer measurements served to define a mean and mode for each rock unit tested (Table 3, Figure 7). These data yield a bimodal distribution of rock strengths (R values). The older, predominately sandstone rocks exposed at higher elevations in the western part of the range have a mean Schmidt value and standard error of 43.8 ± 6.1. The younger sandstone, shale, and conglomerate units exposed in the lower half of the western range and in the entire eastern part of the study area have a mean rock strength of 23.4 ± 4.1 (Figure 7). In actuality, the average strength of rock units in the lower half of the range is probably even less than the mean Schmidt value implies because at least one rock unit (Rincon shale) is too weak for the rock strength test (Table 3) and was not included in the calculation.

5.2. Channel Profiles: Concavity and Normalized Steepness Index

[27] The 44 western, low-uplift channels have concavity indices that range between 0.34 and 2.1 (Table 1), with an

Table 3. Relative Rock Strength Data[a]

	El Capitan, Low Uplift			Madranio, High Uplift		
Rock Unit	Mean R	Mode	n	Mean R	Mode	n
Pico	*	*	*	15.2 ± 0.29	15	23
Rincon	below 10	*	20	below 10	*	20
Monterey	34.9 ± 1.0	35	40	30.8 ± 1.6	32	47
Sisquoc	*	*	*	below 10	*	20
Vaqueros	22.7 ± 0.34	20	144	*	*	*
Sespe	20.9 ± 0.35	16	290	*	*	*
Gaviota	**34.2 ± 0.46**	**34**	**341**	*	*	*
Sacate	**55 ± 0.68**	**55.5**	**27**	*	*	*
Matilija	**42.1 ± 1.3**	**40**	**57**	*	*	*

[a]All measurements were taken with a Schmidt hammer device on exposed rocks within or near the channel bed. An asterisk indicates that the rock unit either does not exist in the uplift region or that it was impossible to sample. Roman/boldface text denotes the resistant/less resistant boundary.

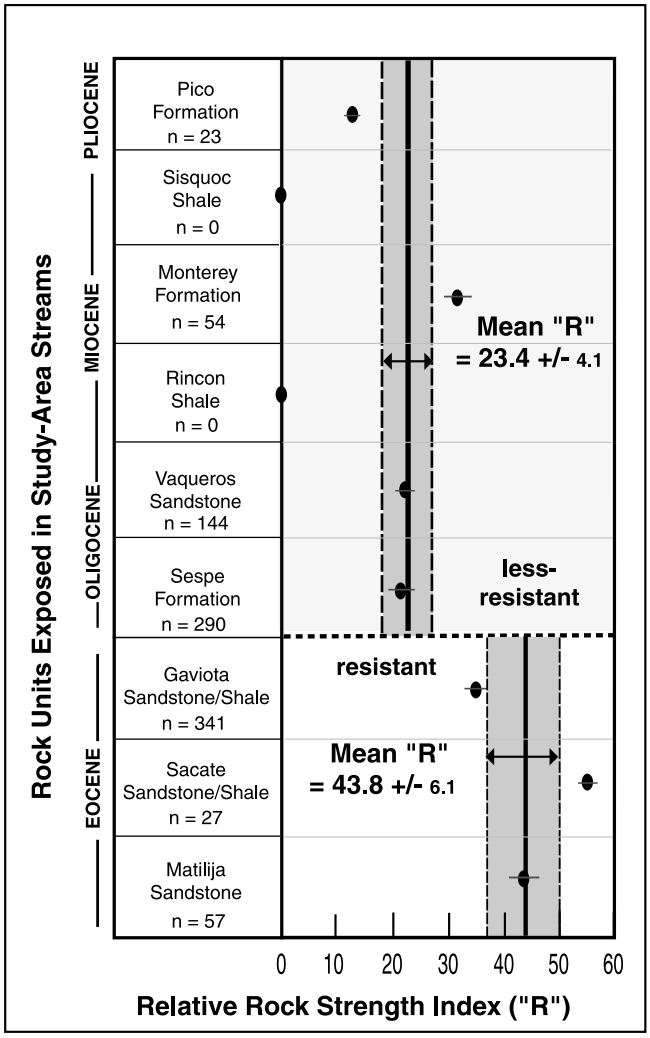

Figure 7. Results of Schmidt hammer test of intact rock strength for rock units exposed in study area streams. The dashed line indicates the boundary of a suite of younger, less resistant rocks (mean *R* value of 23.4) and a suite of older, more resistant rocks that cap the range (mean *R* value of 43.8).

average of 0.83 ± 0.06 (Table 4), a value well above both the theoretically predicted range (0.3–0.6) and results from field sites experiencing uniform rock type and rock uplift [*Snyder et al.*, 2000; *Kirby and Whipple*, 2001]. A key subset of the streams within the region, however, exhibits concavity values within the predicted range (Tables 1 and 4). Nine streams flowing entirely within the weaker Oligocene-Pliocene units along the lower flanks of the range display a mean concavity index of 0.48 ± 0.04. For example, Venadito Canyon (number 34) (Figure 2) has a concavity of 0.4 ± 0.06 (Figure 8, Table 1), whereas the main trunk (east fork) of El Capitan canyon (number 38) (Figure 2), which flows down from near the main drainage divide, has a concavity of 0.81 ± 0.03 (Figure 8, Table 1).

[28] Normalized steepness indices for streams in the low-uplift region exhibit similar differences in response to transitions in rock strength (Table 4). Mean k_{sn} value for channels developed within the weak rock units is 13.8 ± 4.0, whereas the mean value is higher (23.9 ± 1.9) for those streams crossing a transition in rock strength.

[29] Within the high-uplift region, all channels are developed within weak Oligocene-Pliocene units (Table 3). The six channels in the eastern study region exhibit a mean concavity of 0.6 ± 0.09 (Table 4), similar to channels restricted to uniform lithology in the west. The mean normalized steepness index for the high-uplift streams is 26.1 ± 4.9, indicating that channels are ~2–3 times as steep as low-uplift streams in analogous weak rock units (Figure 9).

6. Channel Response to Transitions in Rock Strength

[30] As the results in section 5 demonstrate, channel profiles appear to be strongly influenced by downstream transitions in rock strength in the low-uplift region of the study area. In this section we discuss intrinsic and extrinsic controls on profile concavity and gradient.

6.1. Channel Concavity as a Function of Rock Strength

[31] Concavity indices within our study streams are highly correlated to variability in bedrock competence. Within the weak Oligocene-Pliocene units, channel concavity values fall in a relatively narrow range between ~0.45 and 0.6 and show no strong dependence on rock uplift rate (Tables 1 and 4). Both observations are consistent with theoretical predictions of simple incision models [*Whipple and Tucker*, 1999] and with previous empirical determinations of concavity indices under uniform tectonic forcing and rock type [*Snyder et al.*, 2000; *Kirby and Whipple*, 2001]. Thus we argue that these channels appear to be in equilibrium with the prevailing tectonic forcing.

[32] In contrast, the majority of low-uplift streams have high channel concavities (commonly ≥1). Schmidt hammer tests establish that rocks are stronger toward the crest of the range (mean *R* value of 43.8), whereas lower channel reaches traverse weaker rocks (mean *R* value of 23.4). The 35 streams beginning near the crest of the range yield a mean concavity (θ) of 0.92 ± 0.07, whereas the mean concavity for the 15 streams (both low and high uplift) eroding less resistant rocks along their entire channel length is 0.48 ± 0.04 (Table 4, Figure 10). Thus we attribute the highly concave profiles to this transition from resistant to less resistant rocks.

[33] In an equilibrium system where channels erode at the same rate throughout their entire length, substrate resistance should control channel steepness: Channels will be steeper

Table 4. Summary of Mean Channel Indices

Channel Description	Number of Streams	Concavity[a] (θ)	Steepness Index[a] (k_{sn})
Low-Uplift Region[b]			
Weak rocks only and rock strength transition	43	0.83 (±0.06)	23.9 (±1.9)
Weak rocks only	8	0.48 (±0.04)	13.8 (±4.0)
Rock strength transition only	35	0.92 (±0.07)	26.5 (±2.1)
High-Uplift Region[b]			
Weak rocks only	6	0.6 (±0.09)	26.1 (±4.9)
Weak rocks only	14	0.53 (±0.04)	

[a]Mean values and standard error of the mean (in parentheses) are given.
[b]Low-uplift rate ≈0.75 mm yr^{-1}; high-uplift rate ≈5 mm yr^{-1}.

through resistant rocks and less steep in regions where rocks are weak and easier to erode [*Moglen and Bras*, 1995]. Our results are consistent with this hypothesis. In the Santa Ynez Mountains, channels are steep through the massive sandstone capping the range, whereas in the less resistant units downstream, channel gradients decrease significantly. The combination of a steep upstream reach with a lower-gradient downstream reach creates a composite, highly concave profile. However, we cannot say for certain whether this effect is entirely lithologic; it is possible that the steep upper reaches of these channels also reflect a transient state, where the streams have not yet managed to keep pace with rock uplift. A complete evaluation of this hypothesis awaits additional data on this distribution of incision rate along these channels.

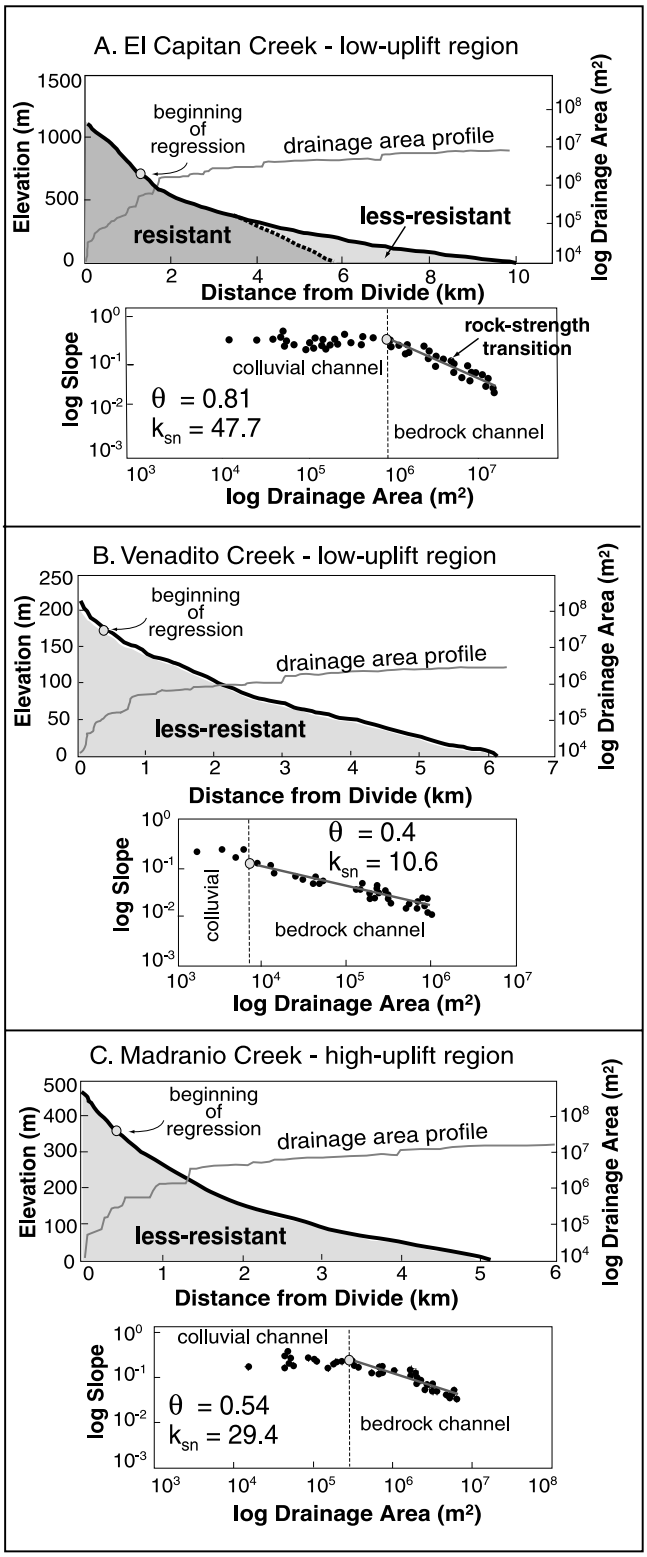

Figure 8. Examples of channel topographic data derived from a digital elevation model: (a) El Capitan creek (number 38), a low-uplift stream that crosses both resistant and less resistant rocks; (b) Venadito creek (number 34), a low-uplift stream draining only weak rocks; and (c) Madranio creek (number 50), a high-uplift stream also eroding only weak rocks. For each stream the top panel shows the channel profile (bold lines) and drainage area (shaded lines) as a function of downstream distance. The shaded circle indicates the beginning of the fluvial part of the channel and the linear regression. The lower panel contains the slope and drainage area data with regression lines. Slopes were calculated at 5 m vertical in elevation intervals.

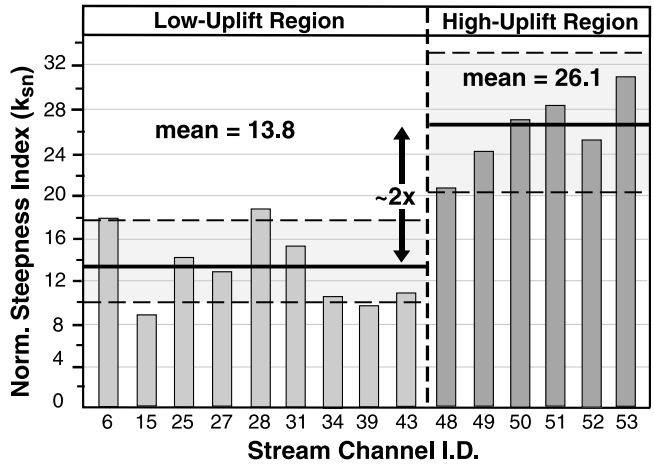

Figure 9. Normalized steepness index (k_{sn}) for all of the weak rock-only channels (identified by stream channel identification number, Figure 2). Mean values and standard error of the mean for each regional data set indicate an approximately twofold increase in k_{sn} in the high-uplift streams.

[34] We draw attention, however, to the smooth transition in gradient area data across this lithologic break (Figure 8a). This behavior is observed in transport-limited models of channel incision [*Whipple and Tucker*, 2002], and it is plausible that such conditions exist in this landscape. However, the degree to which smooth channel profiles across abrupt contrasts in rock strength reflects transport-limited conditions versus sub-reach-scale variations in rock strength and/or the smoothing algorithm used in data processing remains unclear.

6.2. Channel Gradient and the Role of Sediment Transport

[35] One of the more intriguing results of our analysis arises from a comparison of channel gradients between the control set of streams restricted to weak substrate and the

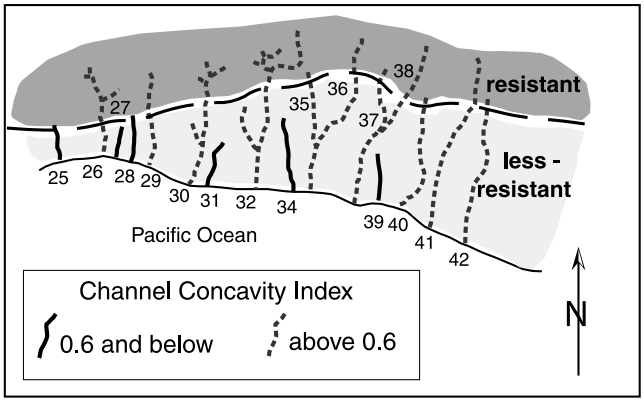

Figure 10. Subset of low-uplift channels (see Figure 1 for regional location), where solid lines depict streams with concavities $\leq$0.6 and dashed shaded lines represent those with concavities >0.6. Note that streams that begin below the transition in rock strength and therefore erode only less resistant rocks have concavities at or below 0.6 (within the predicted range) [*Whipple and Tucker*, 1999], whereas streams experiencing the transition in rock strength have higher concavities.

lower reaches of channels that cross the documented rock strength transition. Despite the larger upstream drainage area, gradients on the lower reaches of high-concavity channels are steeper than gradients on channels developed entirely within the weak substrate (Figure 11). This observation is strikingly inconsistent with the topographic predictions of a simple parameterization of bedrock incision, where larger drainage areas (and thus discharge) should result in lower gradients within the same substrate [e.g., *Whipple and Tucker*, 1999].

[36] One reasonable hypothesis for this behavior is that channel gradients along the high-concavity channels are set by the need to convey sediment derived from resistant bedrock upstream [e.g., *Sklar and Dietrich*, 1998]. The high-gradient lower reaches of these channels are mantled with a discontinuous carpet of coarse (>20 cm) boulders (Figure 3c), most of which comprise resistant sandstone exposed on the upper mountain flanks. Alluvial fans developed at the present-day coastline indicate that most of this material is transported through the length of the channels. In contrast, coarse bed load is uncommon in channels restricted to weak rocks (and without a source of allochthonous resistant sediment) (Figure 3d). The increased gradients along the lower reaches mixed-rock-strength profiles are qualitatively consistent with the predictions of bedrock incision rules that explicitly incorporate a cover effect from sediment [e.g., *Sklar and Dietrich*, 1998, 2001]. Essentially, the transition from hard to weak rocks appears to drive streams toward a transport-limited state, where the size and strength of coarse bed material dictates local channel gradient. If correct, a downstream transition to transport-limited conditions would directly impact the nature and timescale of channel response to variations in tectonic and climatic forcing [e.g., *Whipple and Tucker*, 2002].

7. Channel Response to Tectonic Forcing

[37] Most models for bedrock incision consider that erosion rate is in some manner proportional to mean bed shear stress. It follows intuitively that in an equilibrium system, higher uplift rates require steeper gradients, narrower channels, or some combination of both (for the same discharge) to keep pace with rock uplift [*Whipple et al.*, 1999]. Although both modes of adjustment have been observed [*Lavé and Avouac*, 2000; *Kirby and Whipple*, 2001], the relative role of each process remains highly uncertain [*Snyder et al.*, 2000, 2003a]. Here we examine the response of both channel gradient and width to variable rock uplift rate. We restrict our analysis to only those channels developed in uniform bedrock and thereby circumvent the downstream complexities observed in the mixed-rock-strength channels. Our results suggest that channels adjust both gradient and width in response to tectonic forcing in the Santa Ynez Mountains. Moreover,

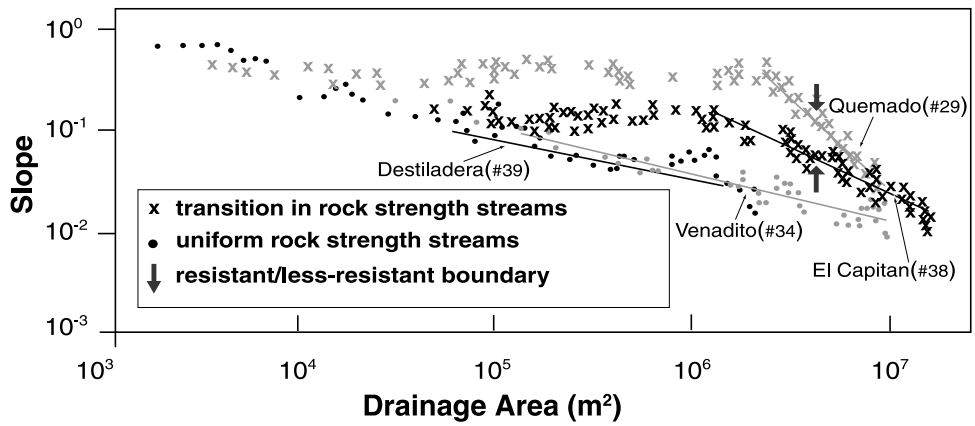

Figure 11. Comparison of channel gradients of low-uplift streams traversing a transition in rock strength (represented by crosses) with those confined to weaker rocks (represented by circles). Arrows indicate where transitions from resistant to less resistant rocks occur. Note that Quemado (number 29) and El Capitan (number 38) (rock strength-transitional streams) are steeper than both Venadito (number 34) and Destiladera (number 39) (streams experiencing uniform rock strength) at the same drainage areas.

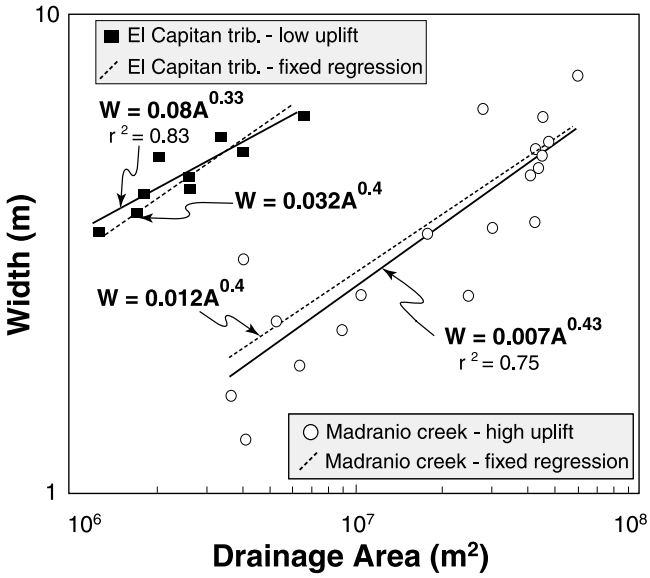

Figure 12. Channel width versus drainage area data for a tributary to El Capitan Creek (number 38) (squares) in the low-uplift region and Madranio Creek (number 50) (circles) in the high-uplift region. Power law regressions through each data set are shown. Channel data for each stream were fixed with an exponent of 0.4 to allow direct comparison of channel width between the two streams. Note that for similar drainage areas the low-uplift stream is ~3 times narrower than the high-uplift stream.

our data set permits a quantitative assessment of key variables within the context of a detachment-limited erosion rule.

7.1. Differences in Channel Width Between Uplift Regions

[38] A clear difference in channel width exists between the low-uplift and high-uplift regions. Regression analysis of data collected from a tributary to El Capitan stream (low-uplift region) yields k'_w of 0.08 and b' of 0.33 (equation (4)), whereas data from Madranio creek (high-uplift region) yields k'_w of 0.007 and b' of 0.42 (Figure 12). Both are similar to observed scaling in bedrock channels [*Montgomery and Gran*, 2001; *Snyder et al.*, 2003a]. In order to effectively compare channel widths at specific drainage areas between these two profiles, we also fit a regression through each data set with $b = 0.4$, equivalent to that approximated by *Montgomery and Gran* [2001]. Results of best fit coefficients indicate a significant narrowing of the high-uplift stream channel (Figure 12). Madranio Creek is ~3 times narrower than the El Capitan tributary at the same drainage area. Schmidt hammer data along with field observations confirm that no obvious differences in rock strength exist between the two catchments (Table 3). Furthermore, climate data from a weather station within the low-uplift region and near the high-uplift streams (Table 5, Figure 1) display negligible differences in mean annual precipitation (<5%) between the two regions, suggesting that regional climate gradients are minimal. Therefore differences in width between the two uplift regions are interpreted to be a result of an increase in rock uplift rate in the eastern part of the study area.

7.2. Empirical Derivation of Channel Parameters *b* and *c*

[39] Typically, values for hydraulic geometry of alluvial rivers (b in equation (4)) are ~0.5 and the basin hydrology exponent (c in equation (4)) ranges between 0.7 and 1 [*Whipple and Tucker*, 1999]. Because channels in uniform substrate exhibit smoothly concave up profiles and display concavity indices consistent with theoretical values, we make the assumption that these channels are in equilibrium with the time-averaged rock uplift rate. Thus we presume that the concavity indices for these channels are a measure of the ratio m/n [*Seidl and Dietrich*, 1992; *Snyder et al.*, 2000; *Kirby and Whipple*, 2001]. Coupled with the empirically derived width data (b'), this ratio allows us to solve for b and c.

[40] Rearranging equation (A8) and utilizing equation (4), we solve for c and b:

$$c = m/n + cb = m/n + b' \tag{5}$$

$$b = 1 - (m/n)c^{-1}. \tag{6}$$

Our results indicate that b is ~0.4 for both the low-uplift and high-uplift regions (Table 6), a value that is consistent with recent work in bedrock channels [*Montgomery and Buffington*, 1997]. The basin hydrology constant c, however, appears to vary between regions. In catchments that experience minimal orographic effects and have a regular shape, c values are expected to be at or close to 1 [*Dunne and Leopold*, 1978]. In this study the high-uplift channels exhibit values of ~1, whereas the low-uplift channels have a somewhat lower value of ~0.8.

[41] Because mean annual precipitation displays a nearly twofold difference between the coast and the range crest [*Warrick*, 2002], we examined theoretical discharge area relationships for a linear, twofold increase in precipitation

Table 5. Mean Annual Precipitation

Water Year	Low Uplift, Western Study Area Precipitation,[a] cm	High Uplift, Eastern Study Area Precipitation,[a] cm	Low/High Ratio
1990	17.98	22.68	0.79
1991	47.45	51.08	0.93
1992	46.91	64.49	0.73
1993	69.75	95.12	0.73
1994	43.97	36.42	1.2
1995	93.98	105.64	0.89
1996	40.84	49.66	0.82
1997	45.57	45.9	0.99
1998	122.48	130.76	0.94
1999	37.44	25.37	1.5
2000	53.98	44.37	1.2
2001	65	51.89	1.3
2002	24.59	19.46	1.3
Mean[b]	**54.61 ± 8.1**	**57.14 ± 9.8**	**1.1**

[a]Precipitation data was recorded using a data logger with tipping bucket and wedge and was taken directly from Santa Barbara County Flood Control District records.

[b]Mean values and standard error are given.

Table 6. Calibrated Channel Parameters[a]

Uplift Region	Empirical			Derived							
	k'_w	b	θ[b]	b	c	n_1[c]	n_2[d]	a_1[c]	a_2[d]	K, $m^{0.26}$ yr^{-1}[e]	K, $m^{0.4}$ yr^{-1}[e]
Low	0.08	0.33	0.5	0.41	0.8	0.62	0.42	0.93	0.42	9.9×10^{-5} ($\pm 1.7 \times 10^{-5}$)	
High	0.007	0.42	0.6	1.0	1.0	0.62	0.42	0.93	0.42		1.5×10^{-4} ($\pm 2.2 \times 10^{-5}$)

[a]Calibrated parameters limited only to channels that do not experience any transitions in rock strength; see list for variable explanations.
[b]We assume $\theta = m/n$ (assumes uniform rock uplift, substrate erodibility, and channel equilibrium).
[c]Calculated assuming shear stress incision rule.
[d]Calculated assuming unit stream power incision rule.
[e]Mean values and standard error (in parentheses) calculated using a range of drainage areas (0.3×10^6–6.5×10^6 m^2).

between the coast and the headwaters. When these climatic gradients are imposed on the short, uniform substrate channels, the resultant variations in c are at most a few percent. Thus it appears that orographic variations in precipitation are unable to account for inferred differences in basin hydrology, and we favor an alternate hypothesis that the hydrology of the catchments varies as a consequence of hillslope character. In the high-uplift region, hillslopes are near threshold values for failures, bare bedrock is exposed along much of the hillslope, and landsliding is common. In the low-uplift region, hillslopes are soil mantled and vegetated, and shallow landslides appear to be less common. We suspect that infiltration and evapotranspiration are greater in this region and that this may account for the differences in our calculated parameter. However, a definitive test of this hypothesis in multiple basins remains to be conducted.

7.3. Differences in Channel Steepness Between Uplift Regions

[42] Given the simple assumption of $n = 1$ and uniform K, the stream power model predicts a linear relationship between the steepness index and rock uplift rate (equation (A19)). Mean values of the steepness index between the high-uplift and low-uplift regions are consistent with the proposition that channels are steeper where rock uplift is more rapid [*Whipple and Tucker*, 1999]. A sixfold to sevenfold increase in rock uplift rate, however, yields only a twofold difference in normalized channel steepness and indicates that one or both of the underlying assumptions (unity of n, uniformity of K) may be invalid. This result was not completely unexpected because channel width also appears to adjust as a function of rock uplift, thereby influencing uniformity in K between uplift regions.

7.4. Empirical Derivation of Channel Parameters *n* and *K* and Constant *a*

[43] The effects of variations in tectonic forcing can be examined by considering a ratio of normalized steepness indices (equation (A19)) between the high-uplift (denoted by a subscript 2) and low-uplift (denoted by a subscript 1) regions [*Snyder et al.*, 2000]:

$$\frac{K_2}{K_1} = \left(\frac{U_2}{U_1}\right)\left(\frac{k_{sn1}}{k_{sn2}}\right)^n, \tag{7}$$

where the ratio of K between the two regions (assuming incision proportional to bed shear stress) is represented by

$$\frac{K_2}{K_1} = \frac{k_{e2}k_{w2}^{-n}k_{q2}^{(1-b_2)n}\rho_w^n g^n}{k_{e1}k_{w1}^{-n}k_{q1}^{(1-b_1)n}\rho_w^n g^n} \tag{8a}$$

or (assuming incision proportional to unit-stream power)

$$\frac{K_2}{K_1} = \frac{k_{e2}k_{w2}^{-3n/2}k_{q2}^{3n/2(1-b_2)}\rho_w^{3n/2} g^{3n/2}}{k_{e1}k_{w1}^{-3n/2}k_{q1}^{3n/2(1-b_2)}\rho_w^{3n/2} g^{3n/2}}. \tag{8b}$$

Presuming that the coefficients representing amount of precipitation (k_q) and rock strength (k_e) are constant between the two sites, and utilizing the result that the width discharge exponent (b) is also roughly constant (Table 6), we can consider adjustment in K as a function of only the hydraulic geometry coefficient (k_w),

$$\frac{K_2}{K_1} = \left(\frac{k_{w2}}{k_{w1}}\right)^{-n} \tag{9a}$$

and

$$\frac{K_2}{K_1} = \left(\frac{k_{w2}}{k_{w1}}\right)^{-3n/2}. \tag{9b}$$

Width versus drainage area comparisons between low-uplift and high-uplift streams (Figure 12) demonstrate variability in channel width between the two regions and can be used to solve for n by substituting the ratio of k_{w2}/k_{w1} into equations (9a) and (9b). Rearrangement to solve for n yields

$$n = \frac{\log\left(\frac{U_2}{U_1}\right)}{\log\left(\frac{k_{w1}k_{sn2}}{k_{w2}k_{sn1}}\right)} \tag{10a}$$

and

$$n = 2/3\left\lfloor\frac{\log\left(\frac{U_2}{U_1}\right)}{\log\left(\frac{k_{w1}k_{sn2}}{k_{w2}k_{sn1}}\right)}\right\rfloor \tag{10b}$$

for the shear stress incision case and unit stream power case, respectively. Values for K within each rock uplift region are found by rearranging the familiar form of detachment-limited bedrock erosion (equation (A5))

$$K = UA^{-m}S^{-n}. \tag{11}$$

Finally, solving for constant a involves only n:

$$a = {}^3\!/_2\, n \tag{12a}$$

and

$$a = n \tag{12b}$$

for shear stress and unit stream power, respectively.

[44] Results from this field site indicate that n is $\sim$0.62 and a is $\sim$0.93 in the shear stress incision case and that both n and a are $\sim$0.42 for the unit stream power rule (Table 6). Theoretically, the slope exponent (n) should be $\sim$2/3 if incision scales linearly with boundary shear stress and $\sim$1 if incision is linear in unit stream power [*Howard and Kerby*, 1983; *Whipple and Tucker*, 1999]. Given that n is $\sim$2/3 in our analysis, whereas n modeled for the unit stream power case (0.42) is significantly lower than theoretically predicted values, we conclude that incision in these streams is better modeled as a function of bed shear stress. Assuming this, we calculated values of K that range from $\sim 9.9 \times 10^{-5}$ ($\pm 1.7 \times 10^{-5}$) $m^{0.26} yr^{-1}$ in the low-uplift region to $\sim 1.5 \times 10^{-4}$ ($\pm 2.2 \times 10^{-5}$) $m^{0.4}$ yr^{-1} in the high-uplift region (Table 6). These values are consistent with prior determinations in similarly weak substrate [*Howard and Kerby*, 1983; *Whipple et al.*, 2000a, 2000b; *Kirby and Whipple*, 2001]. Note that the values differ somewhat from those calculated by *Stock and Montgomery* [1999]; this is a consequence of our choice of parameters m and n.

8. Discussion

[45] One of the outstanding issues currently facing the geomorphic community is to what degree, if any [e.g., *Tomkin et al.*, 2003], do relatively simple rules for bedrock incision by rivers capture the morphologic and dynamic responses of these channels to changes in external forcing. Clearly, whether or not we will be able to draw inferences about the rates and distribution of active deformation directly from channel profile morphology depends on the answer to this overarching question. Our study of bedrock channels draining the Santa Ynez Mountains provides some insight into this problem and suggests that the answer may be neither simple nor unique. In particular, our analysis indicates that a relatively simple channel incision rule works well for a subset of channels in the study area but that it does not adequately describe characteristics of many other channels. We explore the implications of this conclusion below.

[46] We have demonstrated that provided channels are restricted to a uniform lithology and climate, channel incision rate is adequately described as a linear function of boundary shear stress. The success of this simple model, coupled with the observation of relatively uniform channel concavity indices (themselves independent of rock uplift rate), lends support to proposals that channel incision can be parameterized as a function of topographic observables [e.g., *Howard and Kerby*, 1983]. Thus we are encouraged that at least to some degree, local calibration of model parameters can provide useful information regarding channel evolution over geologic time. This result stands in contrast to recent studies [e.g., *Tomkin et al.*, 2003; *van der Beek and Bishop*, 2003] suggesting that the shear stress model is too simplistic a formulation of bedrock incision processes to be of much utility. In particular, *Tomkin et al.* [2003] propose that downstream changes in the effective discharge, a consequence of confined versus unconfined flows, may play an important role. Although we cannot address their hypothesis, we do note that channels in our field site remain in steep-sided gorges out to the coast and do not exhibit broad valleys in their lower reaches.

[47] The success of a simple model in this field site is dependent, however, on the response of channel width to tectonic forcing. One of the most intriguing results of our study is that although we observed a scaling of width with drainage area similar to previous workers [*Montgomery and Gran*, 2001], channel width appears to freely adjust to differences in rock uplift rate. Although adjustments in channel width have been observed in large, gravel-bedded rivers [*Lavé and Avouac*, 2000, 2001], the few studies conducted in bedrock channels of similar size to our study channels did not observe discernable changes in width with rock uplift rate [*Snyder et al.*, 2003a]. Thus our results directly challenge the widespread assumption in landscape evolution models that stream gradient is the only bedrock channel parameter free to adjust to changes in tectonic forcing. Moreover, these results serve to further highlight a critical need for understanding the controls on channel width in bedrock streams [cf. *Whipple*, 2004]. Until we have a rational theory of hydraulic adjustments in bedrock channels, we will be forced to rely on empiricisms such as above.

[48] The apparent adjustment of channel width to rock uplift rate in our study area directly impacts the relationship between channel steepness indices and the rate of tectonic forcing. Although we find that n of $\sim$2/3 can adequately model channel incision, this value predicts that channels experiencing a sixfold to sevenfold difference in rock uplift would exhibit gradient indices 15–18 times larger (assuming uniform K; see equation (A19)). The fact that observed gradient indices in the high-uplift channels are approximately twice that of the low-uplift streams illustrates the dramatic control that channel width can exert on incision rate. Essentially, the effective coefficient of erosion (K) changes in concert with uplift rate in these channels. This result carries the evident implication that in order to glean quantitative information about tectonic forcing from channel profiles, we will need a fuller understanding of the response of channel width [*Lavé and Avouac*, 2000].

[49] Recent studies in the Cape Mendocino region of northern California report similar adjustment of the erosion coefficient to uplift rate [*Snyder et al.*, 2000, 2003a]. In their study, however, these authors attribute the adjustment to the presence of a nonnegligible threshold shear stress for detachment of bedrock [*Snyder et al.*, 2003a]. Although the results of our study do not require an incision threshold to explain the observed channel response, we agree that, intuitively, it is likely that some threshold must be overcome for erosion of the bed to occur. Perhaps, in this field site, the combined effects of weak rocks, long wetting-drying cycles, and intense winter storms are such that any threshold is negligible.

[50] Despite the apparent success of a simple incision model (albeit with variable K) in capturing the response of channels in uniform bedrock to variations in rock uplift rate, the model appears to be unable to explain the observed characteristics of channels traversing the transition in rock strength. First, the change in steepness indices between lower (weak rock) and upper (competent rock) reaches of

these channels is as great, if not greater than, the change in response to a sixfold to sevenfold difference in rock uplift rate. The magnitude of these variations in tectonic forcing are as large as observed in most active orogens, and the fact that lithology can influence channel profiles to such degree is cause for caution in simple interpretation of tectonics from stream profile analysis.

[51] Second, as noted in section 6.2, the increase in gradient (relative to uniform bedrock channels) of the lower reaches of mixed-lithology channels suggests that gradients are dictated by the supply of coarse, competent debris and not by the detachment of local bedrock. Thus we suggest that these channel reaches are probably close to end-member examples of transport-limited bedrock systems [*Whipple and Tucker*, 2002]. Whether these channels are best modeled as entirely transport limited [e.g., *Willgoose et al.*, 1991] or as a hybrid case [e.g., *Sklar and Dietrich*, 1998] is uncertain and awaits a demonstration of steady incision rate across the lithologic boundary. Regardless, the need to invoke different models to describe incision among study area channels implies that a single bedrock incision rule will not capture the entire range of channel behavior observed within this field site. Although the search for a universal model of bedrock incision may be intellectually compelling, perhaps it is fundamentally misguided. Understanding the range of behaviors exhibited by natural systems and the controls of these behaviors may prove to be a more worthy (and attainable) goal.

9. Conclusions

[52] Our study addressed the response of bedrock channel profiles to variations in rock uplift rate and lithology in a site where tectonic forcing and climate are well defined. Several important conclusions regarding both the processes of bedrock channel incision and the potential use of channel profiles as indicators of tectonic forcing are indicated.

[53] 1. Channels developed under conditions of uniform rock uplift rate and lithology display channel concavity indices consistent with the predictions of simple bedrock incision models (θ ranges from 0.3 to 0.6). However, streams that cross transitions in substrate rock strength display dramatic variations in channel profile form.

[54] 2. Streams in the study area appear to adjust both gradient and width in response to increased tectonic forcing. In the high-uplift region, where vertical tectonic rates are roughly 6–7 times that in the low-uplift region, channels are $\sim$2 times as steep and $\sim$3 times as narrow as their low-uplift counterparts.

[55] 3. Empirical calibration of incision model parameters for streams restricted to readily erodible substrate are consistent with previous theoretical and empirical findings in that a is $\sim$1, b is within the range of 0.4–0.6, and c ranges between 0.7 and 1. Values for n, the slope exponent, are $\sim$0.62 and are sufficiently close to the theoretical value of 2/3 to suggest that incision rates scale linearly with boundary shear stress [*Howard and Kerby*, 1983]. The erodibility coefficient (K) is within a range consistent with values found in other field sites with similarly weak rocks.

[56] 4. The erosion coefficient (K) is shown to vary in concert with rock uplift rate, apparently due to a systematic narrowing of channels within the high-uplift region. Thus variability in model parameter K must be considered, even in field sites where rock strength and climate are not known to vary spatially. This suggests caution when trying to draw quantitative inferences regarding the rates and distribution of tectonic forcing directly from channel profiles in the absence of local calibration.

Appendix A

A1. Derivation of Bedrock Channel Incision Rule

[57] In this appendix we review the formulation of a simple detachment-limited incision rule [e.g., *Howard*, 1994]. Both shear stress and unit stream power incision models postulate that the bedrock channel erosion rate (E), in volume per unit channel area per time, is a power law function of the boundary shear stress (τ_b):

$$E = k_b(\tau_b - \tau_c)^a, \tag{A1}$$

where k_b is a dimensional coefficient dependent on dominant erosion process, rock resistance, and possibly sediment load, τ_c is the critical shear stress, a threshold value that must be overcome for incision to occur, and a is a positive, process-dependent constant. The critical shear stress has commonly been neglected in detachment-limited bedrock erosion models because it is assumed that large flood events are responsible for most bedrock erosion and that in these events the boundary shear stress (τ_b) is much greater than the minimum value for incision (τ_c). It should be noted, however, that recent workers [*Tucker and Bras*, 2000; *Snyder et al.*, 2003a, 2003b] have demonstrated the importance of including a nonzero critical shear stress when modeling bedrock erosion. For simplicity we follow previous derivations, which do not specifically include τ_c. Theoretical predictions for the value of constant a range from 1 for a linear erosion process in weak material [*Howard and Kerby*, 1983] to $\sim$5/2 for impact abrasion by sediment [*Foley*, 1980; *Hancock et al.*, 1998; *Whipple et al.*, 2000a]. Assuming conservation of mass (water), and steady, uniform flow, then the boundary shear stress can be written as

$$\tau_b = \rho C_f^{1/3}\left[\frac{gSQ}{W}\right]^{2/3}, \tag{A2}$$

where ρ is density of water, C_f is a dimensionless friction factor, g is gravitational acceleration, S is local channel slope (d_z/d_x), Q is a characteristic stream discharge [*Wolman and Miller*, 1960], and W is a characteristic channel width.

[58] Two basic assumptions regarding hydraulic geometry of the channel are often substituted into equation (A2). First, a relationship for basin hydrology is assumed:

$$Q = k_q A^c, \tag{A3}$$

where A is upstream drainage area, k_q is a dimensional coefficient, and c is a positive constant, the value of which ranges from 0.7 to 1 but which is approximately unity for regularly shaped basins with minimal orographic effects [*Dunne and Leopold*, 1978; *Pazzaglia et al.*, 1998]. Second,

a relationship between channel width and discharge is assumed and combined with equation (A3):

$$W = k_w Q^b = k_w k_q^b A^{bc}, \tag{A4}$$

where k_w is a dimensional coefficient and b is a positive constant, empirically observed to be ~0.5 in both alluvial [*Leopold and Maddock*, 1953] and bedrock rivers [*Montgomery and Gran*, 2001]. Combining equations (A1)–(A4), we obtain the commonly stated "shear stress" incision law [*Howard and Kerby*, 1983; *Howard et al.*, 1994]:

$$E = KA^m S^n, \tag{A5}$$

where m and n are positive constants and K is a dimensional coefficient of erosion. Variables in equation (1) represent the specific relations [*Whipple and Tucker*, 1999]

$$m = (2ac/3)(1 - b); \tag{A6}$$

$$n = 2a/3; \tag{A7}$$

$$m/n = c(1 - b); \tag{A8}$$

$$K = k_e k_w^{-n} k_q^{n(1-b)} \rho^{3n/2} g^n. \tag{A9}$$

Similar results are found in the unit stream power case [*Whipple and Tucker*, 1999]:

$$m = ac(1 - b); \tag{A10}$$

$$n = a; \tag{A11}$$

$$m/n = c(1 - b); \tag{A12}$$

$$K = k_e k_w^{-3n/2} k_q^{3n/2(1-b)} \rho^{3n/2} g^{3n/2}. \tag{A13}$$

[59] Notably, transport-limited incision can be modeled with a similar formulation, where erosion rate is a function of the divergence of volumetric sediment transport capacity [*Willgoose et al.*, 1991; *Tucker and Bras*, 1998; *Whipple and Tucker*, 2002]:

$$Q_c = K_t A^{m_t} S^{n_t}, \tag{A14}$$

where K_t is a dimensional transport coefficient and m_t and n_t are positive constants.

A2. Equilibrium Profiles

[60] The evolution of bedrock channel profiles is commonly posed as a competition between rock uplift and erosion [*Howard*, 1994; *Whipple and Tucker*, 1999]:

$$\partial z/\partial t = U(x,t) - KA^m S^n, \tag{A15}$$

where $[\partial z/\partial t]$ is the time rate of change of bed elevation, U is the rock uplift rate relative to a fixed base level, and erosion rate is modeled as described in section A1 (equation (A5)).

[61] For fluvial landscapes where erosion balances rock uplift everywhere along the channel (i.e., channel equilibrium) and under conditions of spatially uniform uplift, rock strength, and erosion process, equation (A15) can be solved for the equilibrium channel gradient (S_e):

$$S_e = (U/K)^{1/n} A^{-m/n}. \tag{A16}$$

Under the above-stated restrictive conditions of uniform U and K the ratio of m/n sets the rate of change of channel gradient with drainage area, and the coefficient $(U/K)^{1/n}$ dictates equilibrium profile steepness. Previous empirical studies, carried out in a wide variety of geologic settings, reveal power function relations similar in form to equation (A16) that describe stream gradient as

$$S = k_s A^{-\theta}, \tag{A17}$$

with the implied relations

$$\theta = m/n \tag{A18}$$

and

$$k_s = (U/K)^{1/n}. \tag{A19}$$

[62] Regressions of channel gradient and drainage area data readily provide a direct estimate of both θ (the concavity index) and k_s (referred to as the normalized steepness index, k_{sn}) from stream profiles [*Snyder et al.*, 2000; *Kirby and Whipple*, 2001]. Stream channel concavity (θ) is the downstream rate of change of slope with respect to drainage area (Figure 5b). Theoretical predictions indicate that channel concavities should fall within a range of 0.30–0.60 given a uniform rock uplift rate, rock erodibility, and climate [*Whipple and Tucker*, 1999; *Roe et al.*, 2002], and previous empirical studies have found similar results [*Hack*, 1957; *Tarboton et al.*, 1991; *Moglen and Bras*, 1995; *Slingerland et al.*, 1998]. A normalized steepness index (k_{sn}) has been utilized in several recent studies [*Snyder et al.*, 2000; *Kirby and Whipple*, 2001; *Kirby et al.*, 2003] and is a generalized form of the stream gradient index developed by *Hack* [1973]. This relative measure of channel gradient is useful for comparison of profile gradient among multiple channels. Caution must be applied when analyzing stream longitudinal profiles because equations (A18) and (A19) only hold true under a very specific set of conditions. Namely, the river profile must be in steady state with respect to both climatic and rock uplift conditions, and rock uplift rate (U) and the coefficient of erosion (K) must be uniform along the entire channel reach. Only when these conditions are met can $(U/K)^{1/n}$ and m/n be estimated directly from regressions of channel data.

[63] **Acknowledgments.** This research was conducted with support from the USGS National Earthquake Hazard Reduction Program to E. Kirby and D. Burbank (03HQJR0051) and a Geological Society of America graduate student research award to A. Duvall (7130-02). We wish to thank Coast Ranch and the El Capitan Canyon Resort for granting us access to

channels on their property, without which much of this work would not have been possible. We thank Kelin Whipple and two anonymous reviewers for thoughtful and constructive reviews. We also acknowledge Mike Oskin, Manny Gabet, and Nathan Niemi for programming assistance and useful discussion. We must also recognize a very long list of field assistants, for which individual names are too numerous to mention.

References

Anderson, R. S. (1994), Evolution of the Santa Cruz Mountains, California, through tectonic growth and geomorphic decay, *J. Geophys. Res.*, *99*, 20,161–20,179.

Burbank, D. W., J. Leland, E. Fielding, R. S. Anderson, N. Brozovic, M. R. Reid, and C. Duncan (1996), Bedrock incision, rock uplift and threshold hillslopes in the northwestern Himalayas, *Nature*, *379*, 505–510.

Dibblee, T. W., Jr. (1982), Regional geology of the Transverse Ranges province of southern California, in *Geology and Mineral Wealth of the California Transverse Ranges*, edited by D. L. Fife and J. L. Minch, pp. 27–39, South Coast Geol. Soc., Santa Ana, Calif.

Dunne, T., and L. B. Leopold (1978), *Water in Environmental Planning*, 818 pp., W. H. Freeman, New York.

Flint, J. J. (1974), Stream gradient as a function of order, magnitude, and discharge, *Water Resour. Res.*, *10*, 969–973.

Foley, M. (1980), Bed-rock incision by streams, *GSA Bull.*, *91*, 2189–2213.

Gurrola, L. D., E. A. Keller, M. A. Trecker, R. D. Hartleb, and T. W. Dibblee (1998), Active folding and reverse faulting, Santa Barbara fold belt, California, in *Field Trip Guidebook, 94th Annual Meeting, Cordilleran Section*, edited by R. Behl, pp. 1–43, Geol. Soc. of Am., Boulder, Colo.

Hack, J. T. (1957), Studies of longitudinal stream profiles in Virginia and Maryland, *U.S. Geol. Surv. Prof. Pap.*, *294-B*, 45–97.

Hack, J. T. (1973), Stream-profile analysis and stream-gradient indices, *J. Res. U.S. Geol. Surv.*, *1*, 421–429.

Hancock, G. S., and R. S. Anderson (2002), Numerical modeling of fluvial terrace formation in response to oscillating climate, *Geol. Soc. Am. Bull.*, *114*, 1131–1142.

Hancock, G. S., R. S. Anderson, and K. X. Whipple (1998), Beyond power: Bedrock river incision process and form, in *Rivers Over Rock: Fluvial Processes in Bedrock Channels*, *Geophys. Monogr. Ser.*, vol. 107, edited by K. J. Tinkler and E. E. Wohl, pp. 35–60, AGU, Washington, D. C.

Harbor, D. J. (1998), Dynamic equilibrium between an active uplift and the Sevier River, Utah, *J. Geol.*, *196*, 181–198.

Howard, A. D. (1994), A detachment-limited model of drainage basin evolution, *Water Resour. Res.*, *30*, 2261–2285.

Howard, A. D., and G. Kerby (1983), Channel changes in badlands, *Geol. Soc. Am. Bull.*, *94*, 739–752.

Howard, A. D., W. E. Dietrich, and M. A. Seidl (1994), Modeling fluvial erosion on regional to continental scales, *J. Geophys. Res.*, *99*, 13,971–13,986.

Keller, E. A. (1986), Investigation of active tectonics: Use of surficial Earth processes, in *Active Tectonics*, pp. 136–147, Natl. Academy Press, Washington, D. C.

Keller, E. A., and L. D. Gurrola (2000), Earthquake hazard of the Santa Barbara fold belt, California, final report, 106 pp., Inst. for Crustal Stud., Santa Barbara, Calif.

Kirby, E., and K. Whipple (2001), Quantifying differential rock-uplift rates via stream profile analysis, *Geology*, *29*(5), 415–418.

Kirby, E., K. X. Whipple, W. Tang, and C. Zhiliang (2003), Distribution of active rock uplift along the eastern margin of the Tibetan Plateau: Inferences from bedrock channel longitudinal profiles, *J. Geophys. Res.*, *108*(B4), 2217, doi:10.1029/2001JB000861.

Lambeck, K., and J. Chappell (2001), Sea level change through the last glacial cycle, *Science*, *292*, 679–686.

Lavé, J., and J. P. Avouac (2000), Active folding of fluvial terraces across the Siwalik Hills, Himalayas of central Nepal, *J. Geophys. Res.*, *105*, 5735–5770.

Lavé, J., and J. P. Avouac (2001), Fluvial incision and tectonic uplift across the Himalayas of central Nepal, *J. Geophys. Res.*, *106*, 26,561–26,591.

Leopold, L. B., and T. Maddock (1953), Hydraulic geometry of streams and some physiographic implications, *U.S. Geol. Surv. Prof. Pap.*, *252*, 57 pp.

Merritts, D., and K. R. Vincent (1989), Geomorphic response of coastal streams to low, intermediate and high rates of uplift, Mendocino triple junction region, northern California, *Geol. Soc. Am. Bull.*, *101*, 1373–1388.

Metcalf, J. G. (1994), Morphology, chronology, and deformation of Pleistocene marine terraces, southwestern Santa Barbara County, California, M.S. thesis, Univ. of Calif., Santa Barbara.

Moglen, G. E., and R. L. Bras (1995), The effect of spatial heterogeneities on geomorphic expression in a model of basin evolution, *Water Resour. Res.*, *31*, 2613–2623.

Montgomery, D. R., and M. Brandon (2002), Topographic controls on erosion rates in tectonically active mountain ranges, *Earth Planet. Sci. Lett.*, *201*, 481–489.

Montgomery, D. R., and J. M. Buffington (1997), Channel-reach morphology in mountain drainage basins, *Geol. Soc. Am. Bull.*, *109*, 596–611.

Montgomery, D. R., and K. B. Gran (2001), Downstream variations in the width of bedrock channels, *Water Resour. Res.*, *37*, 1841–1846.

Pazzaglia, F. J., T. W. Gardner, and D. J. Merritts (1998), Bedrock fluvial incision and longitudinal profile development over geologic time scales determined by fluvial terraces, in *Rivers Over Rock: Fluvial Processes in Bedrock Channels*, *Geophys. Monogr. Ser.*, vol. 107, edited by K. J. Tinkler and E. E. Wohl, pp. 207–235, AGU, Washington, D. C.

Rockwell, T. K., J. Nolan, D. L. Johnson, and R. H. Patterson (1992), Ages and deformation of marine terraces between Point Conception and Gaviota, Western Transverse Ranges, California, in *Quaternary Coasts of the United States: Marine and Lacustrine Systems*, edited by J. F. Wehmiller and C. Fletcher, pp. 333–341, Soc. of Econ. Paleontol. and Mineral., Tulsa, Okla.

Roe, G. H., D. R. Montgomery, and B. Hallet (2002), Effects of orographic precipitation variations on the concavity of steady-state river profiles, *Geology*, *30*(2), 143–146.

Roe, G. H., D. R. Montgomery, and B. Hallet (2003), Orographic precipitation and the relief of mountain ranges, *J. Geophys. Res.*, *108*(B6), 2315, doi:10.1029/2001JB001521.

Rosenbloom, N. A., and R. S. Anderson (1994), Hillslope and channel evolution in a marine terraced landscape, Santa Cruz, California, *J. Geophys. Res.*, *99*, 14,013–14,029.

Schmidt, K. M., and D. R. Montgomery (1995), Limits to relief, *Science*, *270*, 617–620.

Schumm, S. A., J. F. Dumont, and J. M. Holbrook (2000), *Active Tectonics and Alluvial Rivers*, 276 pp., Cambridge Univ. Press, New York.

Seeber, L., and V. Gornitz (1983), River profiles along the Himalayan arc as indicators of active tectonics, *Tectonophysics*, *92*, 335–367.

Seidl, M. A., and W. E. Dietrich (1992), The problem of channel erosion into bedrock, *Catena*, *23*, suppl., 101–124.

Seidl, M. A., W. E. Dietrich, and J. W. Kirchner (1994), Longitudinal profile development into bedrock: An analysis of Hawaiian channels, *J. Geol.*, *102*, 457–474.

Selby, M. J. (1982), *Hillslope Materials and Processes*, 264 pp., Oxford Univ. Press, New York.

Sklar, L., and W. E. Dietrich (1998), River longitudinal profiles and bedrock incision models: Stream power and the influence of sediment supply, in *Rivers Over Rock: Fluvial Processes in Bedrock Channels*, *Geophys. Monogr. Ser.*, vol. 107, edited by K. J. Tinkler and E. E. Wohl, pp. 237–260, AGU, Washington, D. C.

Sklar, L. S., and W. E. Dietrich (2001), Sediment and rock strength controls on river incision into bedrock, *Geology*, *29*(12), 1087–1090.

Slingerland, R., S. D. Willett, and N. Hovius (1998), Slope-area scaling as a test of fluvial bedrock erosion laws (abstract), *Eos Trans. AGU*, *79*(45), Fall Meet. Suppl., F358.

Snyder, N. P., K. X. Whipple, G. E. Tucker, and D. J. Merritts (2000), Landscape response to tectonic forcing: Digital elevation model analysis of stream profiles in the Mendocino triple junction region, northern California, *Geol. Soc. Am. Bull.*, *112*, 1250–1263.

Snyder, N. P., K. X. Whipple, G. E. Tucker, and D. J. Merritts (2003a), Channel response to tectonic forcing: Field analysis of stream morphology and hydrology in the Mendocino triple junction region, northern California, *Geomorphology*, *53*, 97–127.

Snyder, N. P., K. X. Whipple, G. E. Tucker, and D. J. Merritts (2003b), Importance of a stochastic distribution of floods and erosion thresholds in the bedrock river incision problem, *J. Geophys. Res.*, *108*(B2), 2117, doi:10.1029/2001JB001655.

Stock, J. D., and W. E. Dietrich (2003), Valley incision by debris flows: Evidence of a topographic signature, *Water Resour. Res.*, *39*(4), 1089, doi:10.1029/2001WR001057.

Stock, J. D., and D. R. Montgomery (1999), Geologic constraints on bedrock river incision using the stream power law, *J. Geophys. Res.*, *104*, 4983–4993.

Tarboton, D. G., R. L. Bras, and I. Rodriguez-Iturbe (1991), On the extraction of channel networks from digital elevation data, *Hydrol. Processes*, *5*(1), 81–100.

Tierney, T. E. (2002), Tectonic geomorphology of the greater Santa Ynez Mountains, Santa Barbara County, California, M.S. thesis, Univ. of Calif., Santa Barbara.

Tinkler, K. J., , and E. E. Wohl (Eds.) (1998), *Rivers Over Rock: Fluvial Processes in Bedrock Channels*, *Geophys. Monogr. Ser.*, vol. 107, 323 pp., AGU, Washington, D. C.

Tomkin, J. H., M. T. Brandon, F. J. Pazzaglia, J. R. Barbour, and S. D. Willett (2003), Quantitative testing of bedrock incision models for the

Clearwater River, NW Washington State, *J. Geophys. Res.*, *108*(B6), 2308, doi:10.1029/2001JB000862.

Trecker, M. A., L. D. Gurrola, and E. A. Keller (1998), Oxygen-isotope correlation of marine terraces and uplift of the Mesa Hills, Santa Barbara, California, USA, *Geol. Soc. Spec. Publ.*, *146*, 57–69.

Tucker, G. E., and R. L. Bras (1998), Hillslope processes, drainage density, and landscape morphology, *Water Resour. Res.*, *34*, 2751–2764.

Tucker, G. E., and R. L. Bras (2000), A stochastic approach to modeling the role of rainfall variability in drainage basin evolution, *Water Resour. Res.*, *36*, 1953–1964.

Tucker, G. E., and R. Slingerland (1996), Predicting sediment flux from fold and thrust belts, *Basin Res.*, *8*, 329–349.

van der Beek, P., and P. Bishop (2003), Cenozoic river profile development in the Upper Lachlan catchment (SE Australia) as a test of quantitative fluvial incision models, *J. Geophys. Res.*, *108*(B6), 2309, doi:10.1029/2002JB002125.

Warrick, J. A. (2002), Short-term (1997–2000) and long-term (1928–2000) observations of river water and sediment discharge to the Santa Barbara Channel, California, report, Univ. of Calif., Santa Barbara.

Whipple, K. X. (2004), Bedrock rivers and the geomorphology of active orogens, *Ann. Rev. Earth Planet. Sci.*, *32*, 151–185.

Whipple, K. X., and G. E. Tucker (1999), Dynamics of the stream-power river incision model: Implications for height limits of mountain ranges, landscape response timescales, and research needs, *J. Geophys. Res.*, *104*, 17,661–17,674.

Whipple, K. X., and G. E. Tucker (2002), Implications of sediment-flux-dependent river incision models for landscape evolution, *J. Geophys. Res.*, *107*(B2), 2039, doi:10.1029/2000JB000044.

Whipple, K. E., E. Kirby, and S. H. Brocklehurst (1999), Geomorphic limits to climate-induced increases in topographic relief, *Nature*, *401*, 39–43.

Whipple, K. X., G. S. Hancock, and R. S. Anderson (2000a), River incision into bedrock: Mechanics and relative efficacy of plucking, abrasion, and cavitation, *Geol. Soc. Am. Bull.*, *112*, 490–503.

Whipple, K. X., N. P. Snyder, and K. Dollenmayer (2000b), Rates and processes of bedrock incision by the Upper Ukak River since the 1912 Novarupta ash flow in the Valley of Ten Thousand Smokes, *Alaska, Geology*, *28*(9), 835–838.

Willett, S. D. (1999), Orogeny and orography: The effects of erosion on the structure of mountain belts, *J. Geophys. Res.*, *104*, 28,957–28,982.

Willgoose, G. (1994), A physical explanation for an observed-slope-elevation relationship for catchments with declining relief, *Water Resour. Res.*, *30*, 151–159.

Willgoose, G., R. L. Bras, and I. Rodriguez-Iturbe (1991), Results from a new model of river basin evolution, *Earth Surf. Processes Landforms*, *16*, 237–254.

Wolman, M. G., and J. P. Miller (1960), Magnitude and frequency of forces in geomorphic processes, *J. Geol.*, *68*, 54–74.

D. Burbank, Department of Geological Sciences, University of California, Santa Barbara, CA 93111, USA. (burbank@crustal.ucsb.edu)

A. Duvall, U.S. Geological Survey, MS 973, 345 Middlefield Road, Menlo Park, CA 94025, USA. (aduvall@usgs.gov)

E. Kirby, Department of Geosciences, Pennsylvania State University, University Park, PA 16802, USA. (ekirby@geosc.psu.edu)